A Gaussian filtering method for multi-target tracking with nonlinear/non-Gaussian measurements

Ángel F. García-Fernández, Jason Ralph, Paul Horridge, Simon Maskell

***Abstract*—This paper proposes a Gaussian filtering method to approximate the single-target updates and normalising constants for multi-target tracking with nonlinear, non-Gaussian measurements and a state-dependent probability of detection. The Gaussian approximation is based on the posterior linearisation technique, which seeks the optimal affine approximation of the nonlinearities in a mean square error sense. The normalising constant is approximated using sigma-points based on the posterior. The proposed approach is implemented in a Poisson multi-Bernoulli mixture filter and compared against standard methods to approximate single-target posteriors and normalising constants in two range-bearings tracking scenarios.**

***Index Terms*—Multiple target tracking, state-dependent detection probability, non-linear non-Gaussian measurements.**

I. Introduction

In many applications, it is important to obtain information on multiple targets present in an area of interest based on noisy sensor measurements. Widely-used sensors for this purpose are radars, lidars, sonars and cameras. The range of applications in which information on multiple targets is relevant is quite broad, including self-driving vehicles [1], unmanned surface vehicles [2], space situational awareness [3] and underwater surveillance [4]. Targets may appear, move and disappear from the scene, so a primary task is to detect and localise the current, unknown set of targets using the available measurements. The main frameworks to solve this task are multiple hypothesis tracking [5], [6], joint probabilistic data association [7] and random finite sets [8]. Relevant connections between these approaches are established in [9], [10].

In Bayesian approaches, all available information on the current set of targets is contained in its posterior density, which refers to the density of the current set of targets given current and past measurements. Under the standard linear/Gaussian measurement and dynamic models, there are closed-form recursions to obtain the required posterior densities in the above frameworks. These posteriors contain data association hypotheses with certain weights and Gaussian single-target densities. If the probability of detection is not constant and measurements are nonlinear and non-Gaussian, it is possible to use particle filtering techniques [11]–[13] and Gaussian approximations to approximate the single-target densities. While particle filters provide asymptotically optimal approximations, this paper focuses on Gaussian approximations, due to their lower computational complexity.

In order to obtain Gaussian single-target densities and represent the multi-target posterior with sufficient precision, the main difficulty lies in the update step. There are three challenges: 1) obtaining accurate Gaussian approximations in nonlinear, non-Gaussian single-target Bayesian updates, 2) approximating the corresponding normalising constants accurately, and 3) accounting for a possibly state-dependent probability of detection.

Gaussian approximations in nonlinear updates can be obtained by the extended Kalman filter (EKF) [14], and sigma-point Kalman filters, such as unscented/cubature/quadrature/linear regression Kalman filters [15]–[20]. These methods are based on performing a certain linearisation of the nonlinear measurement function w.r.t. the prior [14], [19]. However, these methods do not account for the information contained in the received measurements to perform the linearisation. Therefore, these approaches generally work well, but become less accurate for stronger nonlinearities and more informative measurements [21]. The iterated extended Kalman filter takes into account the measurement in the linearisation, but neglects linearisation error [22]. We can take into account the measurement and the linearisation error by making use of statistical linear regression (SLR) of the nonlinear function w.r.t. the posterior [23]. This gives rise to the iterated posterior linearisation filter (IPLF), which is based on iterated SLRs w.r.t. the current Gaussian approximation to the posterior. The IPLF has been generalised in [24] to deal with non-Gaussian measurements, described by their conditional mean and covariance matrix.

The conventional approach to approximating the normalising constant is by evaluating the Gaussian approximation of the measurement density, which was used to obtain the posterior, at the received measurement. For example, this is the case in the Gaussian mixture filters based on the EKF [25] and sigma-points Kalman filters [26], and in the multiple target filters in [27]–[30] [8, Cha. 9]. A state-dependent probability of detection is usually approximated as a constant, fixing its value at the prior mean [8], [31].

The contributions of this paper are the following improvements to how challenges 1)-3) are addressed in the Gaussian multi-target tracking literature. For challenge 1), we first propose the use of the IPLF based on conditional moments. The uncertainty over targets that have never been detected usually spreads over a large area, which implies that their first update is likely to be highly nonlinear [21] and it would take the IPLF several iterations to achieve an accurate approximation.

The authors are with the Department of Electrical Engineering and Electronics, University of Liverpool, Liverpool L69 3GJ, United Kingdom (emails: {angel.garcia-fernandez, jfralph, p.horridge, s.maskell}@liverpool.ac.uk). A. F. García-Fernández is also with the ARIES Research Centre, Universidad Antonio de Nebrija, Madrid, Spain.

The authors would like to thank DSTL Grant no. 1000143726 for financial support.

To speed up its convergence, we propose a measurement-driven initial linearisation, suitable for a class of measurements models. For challenges 2) and 3), we approximate the normalising constant, with state-dependent probability of detection, by drawing sigma-points w.r.t. the posterior approximation. This technique has been used for classification using Gaussian processes in [32] and can be seen as an instance of importance Gaussian quadrature [33].

The paper focuses on the application of the proposed techniques to the Poisson multi-Bernoulli mixture (PMBM) filter [9], [34], which provides the recursion to obtain the posterior with the standard models. We provide simulations in two range-bearings scenarios with von Mises-Fisher (VMF) bearings [35], and with Gaussian and Student's t-range, respectively.

The rest of the paper is organised as follows. Section II introduces the problem formulation. Section III explains how to approximate single-target posteriors. Section IV deals with the approximation of the normalising constant. Simulation results and conclusions are given in Sections V and VI.

II. Problem formulation

We consider the standard multi-target models [8]. Given the set X_k of targets at time step k, each target $x \in X_k$ survives with a probability $p^S(x)$ and moves with transition density $g(\cdot|x)$, or dies with probability $1 - p^S(x)$. New targets are born according to a Poisson point process (PPP) with intensity $\lambda^B(\cdot)$. At time step k, each $x \in X_k$ is detected with a probability $p^D(x)$ and generates a measurement with density $l(\cdot|x)$, or is misdetected with probability $1 - p^D(x)$. Clutter is a PPP with intensity $\lambda^C(\cdot)$. The posterior of X_k can be calculated via the PMBM filter [9], [34].

This paper focuses on approximating the single-target updates, via Gaussian densities, and the normalising constants that arise in the PMBM update. There are two types of single-target updates: detection and misdetection hypotheses. Both are performed for the current targets that have never been detected (represented as a PPP) and, also, for the current targets that have been detected at some point in the past (established tracks) [9]. We drop time indices for notational clarity and proceed to explain the two types of single-target updates.

A. Detection hypotheses

Given the single-target prior

$$p(x) = \mathcal{N}(x; \overline{x}, P), \tag{1}$$

the update with measurement z gives the single-target posterior

$$q_d(x) = \frac{l(z|x)\, p^D(x)\, p(x)}{l(z)} \tag{2}$$

where the normalising constant is

$$l(z) = \int l(z|x)\, p^D(x)\, p(x)\, dx. \tag{3}$$

For nonlinear/non-Gaussian models with a state-dependent $p^D(\cdot)$, (2) and (3) are intractable. Therefore, the objective is to obtain a Gaussian approximation to $q_d(\cdot)$ and an approximation of the normalising constant $l(z)$, which is required to update the weights of the data association hypotheses [6], [9].

B. Misdetection hypotheses

For the update of a misdetection hypothesis with single-target prior (1), the posterior $q_m(\cdot)$ is

$$q_m(x) = \frac{\left(1 - p^D(x)\right) p(x)}{l} \tag{4}$$

where the normalising constant is

$$l = 1 - \int p^D(x)\, p(x)\, dx. \tag{5}$$

If $p^D(\cdot)$ is a constant, the posterior is equal to the prior and $l = 1 - p^D$. However, in general, both (4) and (5) are intractable and approximations are required.

III. Single-target posterior approximation

This section explains a Gaussian approximation of the single-target posterior for detection and misdetection hypotheses, see (2) and (4).

A. Enabling approximation

We obtain a Gaussian approximation to the posterior $q_d(\cdot)$ in (2) using posterior linearisation based on the conditional moments of $l(\cdot|x)$ [23], [24]. The conditional mean and covariance of z given x are written as

$$g(x) = \mathrm{E}[z|x] = \int z l(z|x)\, dz \tag{6}$$

$$R(x) = \mathrm{C}[z|x] = \int (z - g(x))(z - g(x))^T l(z|x)\, dz. \tag{7}$$

Then, we write the relation between z and x as [36]

$$z = g(x) + \eta(x), \tag{8}$$

where $g(x)$ is a nonlinear transformation of x, and $\eta(x)$ is a zero-mean noise with covariance matrix $R(x)$. The noise $\eta(x) = z - g(x)$ is uncorrelated with x and $g(x)$, which means that $\mathrm{C}[x, \eta(x)] = 0$ and $\mathrm{C}[g(x), \eta(x)] = 0$ [37].

To obtain a Gaussian approximation to $q_d(\cdot)$, we make the enabling approximation

$$p^D(x) \approx p^D \tag{9}$$

$$z \approx Ax + b + r \tag{10}$$

where $A \in \mathbb{R}^{n_z \times n_x}$, $b \in \mathbb{R}^{n_z}$ and r is a zero-mean noise with covariance matrix $\Omega \in \mathbb{R}^{n_z \times n_z}$, uncorrelated with x.

It should be noted that (9) implies that Bayes' rule (2) becomes the standard Bayesian update with likelihood $l(z|x)$, irrespective of p^D. The probability of detection has an effect on the normalisation constant approximation, as will be described in Section IV.

Once we make approximation (9)-(10), the linear mean square error estimator and its mean square error matrix are available in closed-form and can be used to approximate the first two moments of the posterior [37]. Under the additional

assumption that r is Gaussian, the posterior approximation $\hat{q}_d(\cdot)$ becomes Gaussian with mean and covariance matrix provided by the (affine) Kalman filter update [18]

$$\overline{u} = \overline{x} + PA^T \left(APA^T + \Omega\right)^{-1} (z - A\overline{x} - b), \quad (11)$$

$$W = P - PA^T \left(APA^T + \Omega\right)^{-1} AP. \quad (12)$$

Therefore, under the enabling approximation (9)-(10), the accuracy of the posterior approximation $\hat{q}_d(\cdot)$ for detection hypotheses only depends on the choice A, b and Ω. Different choices of these parameters give rise to different filters [23, Sec. II.A]. The selection of these parameters for the IPLF is addressed in Section III-B.

For misdetection hypotheses, there is no measurement, and the posterior is given by (4). Therefore, the enabling approximation is just (9), which implies that the posterior approximation is equal to the prior (1).

B. Posterior linearisation filter

In this section, we explain how we select (10). A standard approach is via Taylor series linearisation of the measurement function around the prior mean, as in the EKF, or via SLR w.r.t. to the prior, which can be approximated using sigma-points, as in the unscented and cubature Kalman filters. For a detailed description on the choice of (10) for these filters, we refer the reader to [23, Sec. II.A]. Linearising w.r.t. the prior in either form is inaccurate if measurement nonlinearities are sufficiently large in comparison with the measurement noise covariance matrix [21].

If the prior uncertainties are sufficiently small, measurement nonlinearities in the area of the prior are usually small, and nonlinear Kalman filters based on prior linearisation work well. However, the spatial uncertainty for undetected targets (PPP component of the PMBM filter) usually covers the whole surveillance area, as new born targets can usually appear at any point. In this case, nonlinearities in the detection update can be significant, and standard nonlinear Kalman filters based on the prior will not approximate (2) accurately.

To solve the problem of high nonlinearities and be able to deal with measurement models of the type (8), we use the posterior linearisation filter based on conditional moments in [24]. We first review the concept of the generalised SLR.

1) Statistical linear regression: Given a density $p(\cdot)$ on x, with mean $\overline{x}$ and covariance matrix P, and a measurement model (8), SLR provides A^+ and b^+ that minimise the mean square error of $g(x) + \eta(x)$ and its affine approximation

$$\left(A^+, b^+\right) = \underset{(A,b)}{\arg\min}\, \mathrm{E}\left[\left\|g(x) + \eta(x) - Ax - b\right\|^2\right] \quad (13)$$

$$= \underset{(A,b)}{\arg\min}\, \mathrm{E}\left[\left\|g(x) - Ax - b\right\|^2\right], \quad (14)$$

where we have used in (14) that $g(x)$ and $\eta(x)$ are uncorrelated. This yields [24]

$$A^+ = \mathrm{C}\left[x, g(x)\right]^T P^{-1}, \quad (15)$$

$$b^+ = \mathrm{E}\left[g(x)\right] - A^+ \overline{x}. \quad (16)$$

The resulting mean square error matrix is

$$\Omega^+ = \mathrm{E}\left[\left(g(x) - A^+x - b^+\right)\left(g(x) - A^+x - b^+\right)^T\right] + \mathrm{E}\left[\eta(x)\,\eta^T(x)\right] \quad (17)$$

$$= \mathrm{C}\left[g(x)\right] + \mathrm{E}\left[R(x)\right] - A^+P\left(A^+\right)^T. \quad (18)$$

The moments $\mathrm{E}\left[g(x)\right]$, $\mathrm{C}\left[x, g(x)\right]$, $\mathrm{C}\left[g(x)\right]$ and $\mathrm{E}\left[R(x)\right]$ can be approximated using sigma-points w.r.t. density $p(\cdot)$ or by first-order Taylor series linearisation [24, Sec. III].

2) Iterated posterior linearisation filter: The idea of posterior linearisation is that, to account for the information contained in the measurement, we should condition on z in (14) and (18). This provides us with the best linearisation in a mean square error sense given z, and the resulting linearisation is given by SLR w.r.t. the posterior. This approach cannot be applied directly because we require knowledge of the posterior to approximate the posterior. Nevertheless, it is useful to design an iterated algorithm, in which we perform iterated SLRs w.r.t., the best available approximation to the posterior, giving rise to the IPLF.

In the IPLF, we start with the prior $\overline{u}^1 = \overline{x}$, $W^1 = P$ and calculate the SLR parameters A^1, b^1, Ω^1 w.r.t. a density with moments $\overline{u}^1$ and W^1, using (15)-(18). Then, we substitute A^1, b^1, Ω^1 into (11) and (12) to obtain $\overline{u}^2$ and W^2. Subsequently, we calculate the SLR A^2, b^2, Ω^2 w.r.t. $\overline{u}^2$ and W^2. The iteration continues for a fixed number of steps or until a convergence criterion is met, for example, if the Kullback-Leibler divergence between the Gaussian posterior approximations at two consecutive iterations is lower than a threshold [23, Sec. IV.D].

3) Measurement driven linearisation: As mentioned at the beginning of Section III-B, the nonlinearities will most severely affect the detection hypothesis of targets that have never been detected. In this setting, it may take the IPLF several steps to reach a suitable linearisation and there is a higher risk of divergence. For this update, we propose a measurement driven initial linearisation. A related approach for particle-based methods is explained in [38]. That is, rather than starting the SLR iterations w.r.t. the prior (1), we perform the first SLR in the area of the state-space indicated by the measurement.

We write the state vector as $x = \left[x_a^T, x_b^T\right]^T$ where $x_a \in \mathbb{R}^{n_a}$ and $x_b \in \mathbb{R}^{n_b}$ with $n_a + n_b = n_x$, $\overline{x} = \left[\overline{x}_a^T, \overline{x}_b^T\right]^T$ and

$$P = \begin{pmatrix} P_{aa} & P_{ab} \\ P_{ab}^T & P_{bb} \end{pmatrix} \quad (19)$$

where P_{aa}, P_{ab} and P_{bb} are the covariance matrices of the partitioning of x into x_a and x_b. We make the assumptions

- A1 The conditional moment $g(x) = g(x_a) = \mathrm{E}\left[z|x_a\right]$ is a bijective function $\mathbb{R}^{n_a} \to \mathbb{R}^{n_z}$.
- A2 The conditional moment $R(x) = \mathrm{C}\left[z|x\right] = R$ is a constant.

Under these assumptions, we can obtain a Gaussian approximation to the likelihood in variable x_a by propagating sigma-points through $g^{-1}(\cdot)$ [39]. That is, given a measurement z, we can draw m sigma-points $\mathcal{Z}_1, ..., \mathcal{Z}_m$ with weights $\omega_1, ..., \omega_m$ that match the moments z and R and obtain the

approximated mean and covariance matrix to approximate $l(z|x_a) \approx \mathcal{N}(z; \overline{a}, A)$ with

$$\overline{a} = \sum_{j=1}^{m} \omega_j \mathcal{A}_j \tag{20}$$

$$A = \sum_{j=1}^{m} \omega_j (\mathcal{A}_j - \overline{a})(\mathcal{A}_j - \overline{a})^T \tag{21}$$

where $\mathcal{A}_j = g^{-1}(\mathcal{Z}_j)$.

Then, using (15)-(18), we perform the SLR of $g(x_a)$ w.r.t. $\mathcal{N}(x_a; \overline{a}, A)$, to yield (A_a, b_a, Ω_a). The considered linearisation parameters at the first IPLF step are $(A^1, b^1, \Omega^1) = ([A_a, 0_{n_z,n_b}], b_a, \Omega_a)$, where $0_{n_z,n_b}$ is a zero matrix of size $n_z \times n_b$, which is appended so that A^1 is of dimensions $n_z \times n_x$.

IV. Normalising constant approximation

This section proposes a method to approximate the normalising constant. We consider detection and misdetection hypotheses in Section IV-A and IV-B, respectively. We also discuss how the algorithm would deal with non-linear/non-Gaussian dynamic models in Section IV-C.

A. Detection hypotheses

The normalising constant (3) for detection hypotheses is

$$l(z) = \mathrm{E}\left[\mathcal{N}(z; h(x), R)\, p^D(x)\right] \tag{22}$$

where the expected value is taken w.r.t. the prior $p(\cdot)$. Apart from Monte Carlo methods, one could compute this integral directly using sigma-points/quadrature/cubature rules, which would imply taking sigma-points w.r.t. the prior $\mathcal{N}(\cdot, \overline{x}, P)$ [15], [18]. If the function $\mathcal{N}(z; h(x), R)\, p^D(x)$ is sufficiently non-linear in the area where $\mathcal{N}(\cdot, \overline{x}, P)$ has its mass, sigma-points may not yield an accurate approximation. This can be specially problematic for large P.

To avoid this drawback, we transform (22) such that we can select sigma points/quadrature points w.r.t. the posterior approximation, whose moments are (11) and (12). The motivation behind this technique is that the posterior approximation has its mass in the region where the integrand in (22) is high and the effect of the nonlinearities is less severe in this area, improving accuracy. This approach bears resemblance to importance sampling, where the samples can be drawn from the posterior approximation [40]. We write (22) as

$$l(z) = \hat{l}(z) \int \frac{l(z|x)}{\hat{l}(z|x)} p^D(x) \frac{\hat{l}(z|x)}{\hat{l}(z)} \mathcal{N}(x, \overline{x}, P)\, dx \tag{23}$$

$$= \hat{l}(z) \int \frac{l(z|x)}{\hat{l}(z|x)} p^D(x)\, \mathcal{N}(x, \overline{u}, W)\, dx \tag{24}$$

where

$$\hat{l}(z) = \mathcal{N}\left(z; A\overline{x} + b, APA^T + \Omega\right) \tag{25}$$

$$\hat{l}(z|x) = \mathcal{N}(z; Ax + b, \Omega). \tag{26}$$

Quantity $\hat{l}(z)$ is the Gaussian approximation to the marginal likelihood (normalising constant), without considering $p^D(\cdot)$, after we make the enabling approximation (10), and $\hat{l}(z|x)$ is the corresponding Gaussian approximation to the conditional density of z given x. The marginal Gaussian likelihood approximation $\hat{l}(z)$ is corrected by the expression inside the integral in (24). By choosing m sigma points $\mathcal{X}_1, ..., \mathcal{X}_m$ and weights $\omega_1, ..., \omega_m$ that match the moments $\overline{u}$ and W according to a suitable sigma-point method [18], the marginal likelihood approximation becomes

$$l(z) \approx \hat{l}(z) \sum_{j=1}^{m} \left[\omega_j \frac{l(z|\mathcal{X}_j)}{\hat{l}(z|\mathcal{X}_j)} p^D(\mathcal{X}_j)\right]. \tag{27}$$

We would like to remark that, just considering the enabling approximation (9)-(10), the normalising constant approximation is

$$l(z) \approx p^D \hat{l}(z). \tag{28}$$

Thus, by comparison of (27) and (28), the enabling approximation (9) that is implicitly used in the calculation (27) is

$$p^D = \sum_{j=1}^{m} \left[\omega_j \frac{l(z|\mathcal{X}_j)}{\hat{l}(z|\mathcal{X}_j)} p^D(\mathcal{X}_j)\right]. \tag{29}$$

We proceed to illustrate the benefits of the proposed approximation of the normalising constant in two examples: one with constant $p^D(\cdot)$ and another with state-dependent $p^D(\cdot)$.

Example 1. Let us consider a Gaussian prior with $\overline{x} = 3$ and $P = 4$, $l(z|x) = \mathcal{N}(z; 0.01x^3, 0.1)$ and $p^D(x) = 1$. In this case, $g(x) = \mathrm{E}[z|x] = 0.01x^3$ and $R(x) = \mathrm{C}[z|x] = 0.1$. We analyse the non-linear Kalman filter (SLR w.r.t. the prior) and the IPLF with 10 steps, both using the analytical expressions of (15)-(18). The obtained posteriors for $z = 1.5$ and the benefits of performing iterated SLRs were illustrated in [23]. Here, we evaluate the accuracy of the following normalising constant approximations:

- Direct nonlinear Kalman filter approximation, which is given by (25) with (A, b, Ω) chosen by SLR w.r.t. the prior. This is the standard normalising constant approximation in nonlinear Gaussian mixture filtering [25], [26].
- Direct IPLF approximation, which is given by (25) with the value of (A, b, Ω) at the last iteration.
- Approximation of (22) using sigma-points w.r.t. the prior.
- Proposed approach: Equation (27), using sigma-points w.r.t. the posterior obtained by the IPLF.

The sigma-points in (27) are chosen according to the Gauss-Hermite quadrature rule [26], which, in a one-dimensional case, coincides with the unscented transform with weight 2/3 for the central sigma-point [15]. The true normalising constant is computed by using a dense grid of points. The true and approximated normalising constants for $z \in [-1, 2]$ are shown in Figure 1. The proposed method based on (27) provides the most accurate approximation.

Example 2. We examine the same scenario and algorithms as in Example 1, but with $p^D(x) = \exp(-|x|/3)$. To compute the normalising constant, the nonlinear Kalman filter and the direct IPLF approximations use the value of $p^D(\cdot)$ at the prior mean $\overline{x}$. The normalising constants are shown in Figure

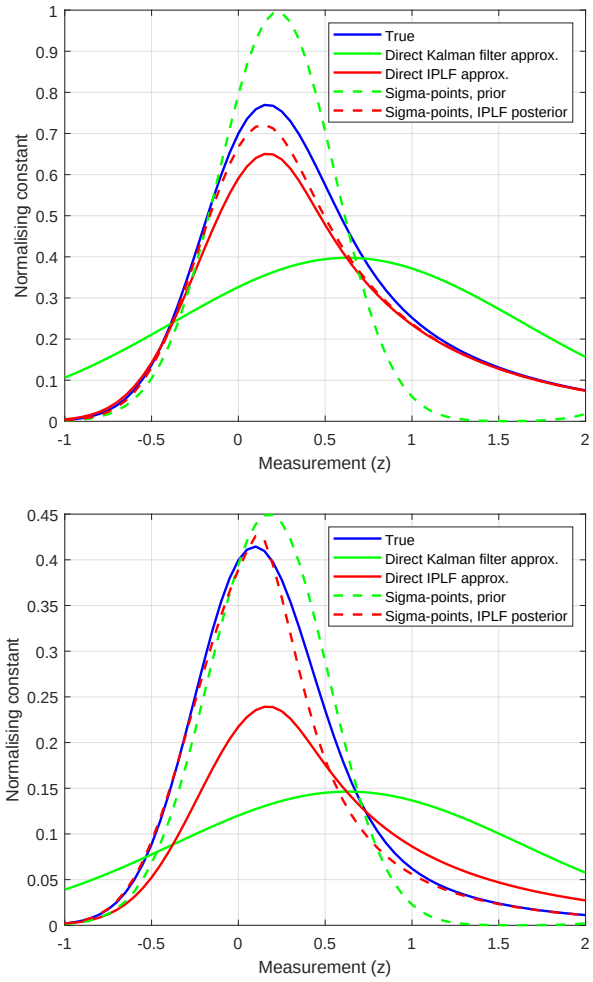

Figure 1: Normalising constants against z in Example 1 (top) and in Example 2 (bottom). The proposed approach based on drawing sigma-points w.r.t. the IPLF posterior, see (27), outperforms the rest. The direct IPLF approximation is accurate in Example 1, but not in Example 2. Drawing sigma-points w.r.t. to the prior to approximate (22) works reasonably well in Example 2, but not in Example 1. The direct nonlinear Kalman filter approximation is considerably less accurate.

1. Approximating the normalising constant drawing sigma-points w.r.t. to the IPLF posterior, using (27), is generally the most accurate algorithm. Drawing the sigma-points w.r.t. the prior, using (22), is also accurate though it performs worse in the right tail. The direct nonlinear Kalman filter and IPLF approximations perform worse.

B. Misdetection hypotheses

The normalising constant for misdetection hypotheses is given by (5) and can be written as

$$l \approx 1 - \mathrm{E}\left[p^D\left(x\right)\right] \tag{30}$$

where the expected value is taken w.r.t. the prior $p\left(\cdot\right)$. In this case, there is no measurement, so we approximate (30) using m sigma points $\mathcal{X}_1, ..., \mathcal{X}_m$ and weights $\omega_1, ..., \omega_m$ that match $\overline{x}$ and P such that

$$l \approx 1 - \sum_{j=1}^{m} \left[\omega_j p^D\left(\mathcal{X}_j\right)\right]. \tag{31}$$

It should be noted that, just considering the enabling approximation (9) for misdetection hypotheses, the normalising constant approximation is

$$l \approx 1 - p^D. \tag{32}$$

Comparing (31) and (32), the enabling approximation (9) that is implicitly used in the calculation (31) is

$$p^D = \sum_{j=1}^{m} \left[\omega_j p^D\left(\mathcal{X}_j\right)\right], \tag{33}$$

which is the expected probability of detection in the area indicated by the prior, approximated by sigma-points.

C. Discussion on the prediction step

In the prediction step, there is no measurement, so one can then proceed similarly as with misdetection hypotheses. We can estimate the average probability of survival using the same approach as in (33). Then, for the single-target predictions, we can use the standard sigma-point Kalman filter prediction step [15] or the generalisation based on conditional moments [24].

V. Simulations

We evaluate different approaches to approximate the single-target posteriors and the normalising constants in a PMBM filter. The method we use to approximate the integrals is the unscented transform with weight 1/3 at the central sigma-point [15], see Appendix A. We use the IPLF with a maximum number of iterations $N_{\text{iplf}} = 1$ and $N_{\text{iplf}} = 5$ and a stopping criterion based on the Kullback-Leibler divergence with threshold 10^{-2} [23, Eq. (30)].

We compare two methods to approximate the normalising constant. The first one is the one proposed in Section IV. The second one is the standard approach in which we approximate the probability of detection at the prior mean $\overline{x}$ and we use the Gaussian approximation to the marginal likelihood, see (25) [8]. That is, for detection hypotheses, we have

$$l\left(z\right) \approx p^D\left(\overline{x}\right) \hat{l}\left(z\right). \tag{34}$$

For misdetection hypotheses, we have

$$l \approx 1 - p^D\left(\overline{x}\right). \tag{35}$$

We also analyse the effect of using a measurement-driven initialisation for the IPLF in newly created Bernoullis. All possible combinations of these approximations give 8 variants of the nonlinear-Gaussian PMBM filters. These variants are identified by the acronym: MxLyNN_{iplf}, where $x = 1$ if we consider measurement driven initialisation and $x = 0$, otherwise, and $y = 1$ if we consider the marginal likelihood (normalising constant) approximation improvement, and $y = 0$ otherwise. Note that the standard approach in the literature, with the unscented Kalman filter and measurement models described by conditional moments [41], corresponds to M0L0N1.

The PMBM filters have been implemented with the following parameters: threshold 10^{-4} for pruning multi-Bernoulli weights, threshold 10^{-5} for pruning PPP components, threshold 10^{-4} for Bernoulli pruning and ellipsoidal gating threshold

50. We also use Murty's algorithm [42] to select the hypotheses with highest weights and the maximum number of global hypotheses is 200. We also consider Estimator 1 with threshold 0.4 [34]. In the rest of the section, all units are given in the international system.

A. Range-bearings measurements

The single-target state is represented as $x = [p_x, v_x, p_y, v_y]^T$ where $[p_x, p_y]^T$ is the position vector and $[v_x, v_y]^T$ is the velocity vector. There is a sensor located at $[s_x, s_y]^T$ that measures direction-of-arrival, represented as a two-dimensional vector z_1 of length 1, and range z_2, such that $z = \left[z_1^T, z_2\right]^T$. The direction-of-arrival measurement z_1 is modelled as a von-Mises Fisher (VMF) distribution [35]

$$l(z_1|x) = \mathcal{V}(z_1; h(x), \kappa) \tag{36}$$

$$h(x) = \frac{[p_x - s_x, p_y - s_y]^T}{r(x)} \tag{37}$$

$$r(x) = \|[p_x - s_x, p_y - s_y]\| \tag{38}$$

where $\mathcal{V}(\cdot; \mu, \kappa)$ is the VMF density embedded in $\mathbb{R}^2$, w.r.t. the uniform distribution, with mean direction μ and concentration parameter $\kappa \geq 0$. This density is

$$\mathcal{V}(z_1; \mu, \kappa) = \frac{\exp\left(\kappa \mu^T z_1\right)}{\mathrm{I}_0(\kappa)} \chi_{\|z_1\|=1}(z_1), \tag{39}$$

where $\mathrm{I}_a(\cdot)$ represents the modified Bessel function of the first kind and order a, $\Gamma(\cdot)$ represents the gamma function and $\chi_A(\cdot)$ is the indicator function on set A. The VMF distribution is unimodal for $\kappa > 0$ and uniform for $\kappa = 0$.

We consider two types of distributions for the range: Gaussian and Student's t-distribution, which has longer tails. For the Gaussian range measurement, the density of z_2 given x is

$$l(z_2|x) = \mathcal{N}(z_2; r(x), R). \tag{40}$$

For the Student's t range measurement, we have

$$l(z_2|x) = \mathrm{S}(z_2; r(x), R, \nu) \tag{41}$$

where $\mathrm{S}(\cdot; \mu, R, \nu)$ denotes a Student's t density with location parameter μ, scale matrix R and ν degrees of freedom [43]

$$\mathrm{S}(z_2; \mu, R, \nu) = \frac{\Gamma[(\nu + p)/2]}{\Gamma[\nu/2]\, \nu^{p/2} \pi^{p/2} |R|^{1/2}} \times \left[1 + \frac{1}{\nu}(z_2 - \mu)^T R^{-1}(z_2 - \mu)\right]^{-(\nu+p)/2} \tag{42}$$

where p is the dimension of the variable z_2, in our case, $p = 1$.

To approximate the single-target posterior and the normalising constant, we need $l(z|x)$, $g(\cdot)$ and $R(\cdot)$. Given the state, the range and direction-of-arrival measurements are independent so

$$l(z|x) = l(z_1|x)\, l(z_2|x) \tag{43}$$

where $l(z_1|x)$ and $l(z_2|x)$ are given by (36), and (40) for Gaussian range or by (41) for Student's t range. The required moments of $g(\cdot)$ and $R(\cdot)$ to perform SLR, see (15)-(18), are provided in Appendix B. In the simulations, we use the parameters $[s_x, s_y]^T = [100, 100]^T$, $\kappa = 1000$, $R = 3$, $\nu = 5$.

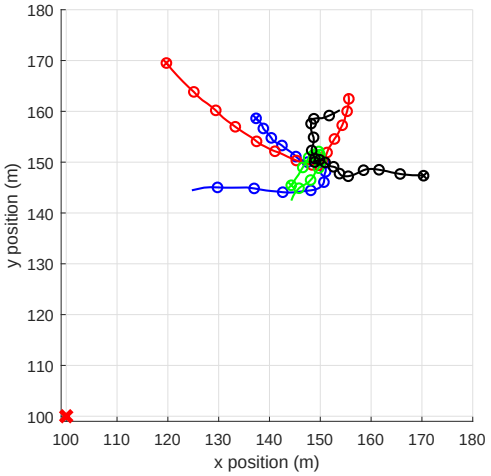

Figure 2: True target trajectories and sensor location (marked with a red cross) in the simulations. Blue, red, green and black targets are born at time steps 5, 1, 10 and 1, and die at time steps 80, 75, 60, 80, respectively. Targets positions every 10 time steps are marked with a circle, and their initial positions with a cross inside the circle. Targets are in close proximity at around time step 40.

B. Multi-target models

Targets move with probability of survival 0.99 and a nearly constant velocity model with transition density

$$g(\cdot|x) = \mathcal{N}(\cdot; Fx, Q) \tag{44}$$

$$F = I_2 \otimes \begin{pmatrix} 1 & \tau \\ 0 & 1 \end{pmatrix}, \; Q = qI_2 \otimes \begin{pmatrix} \tau^3/3 & \tau^2/2 \\ \tau^2/2 & \tau \end{pmatrix} \tag{45}$$

with $\tau = 1$ and $q = 0.01$. The intensity of the PPP birth process is Gaussian with mean $\overline{x}_k^{b,1} = [180, 0, 180, 0]^T$ and covariance matrix $P_k^{b,1} = \mathrm{diag}\left(\left[100^2, 1, 100^2, 1\right]\right)$, with weight $w_1^{b,1} = 1$ for $k = 1$ and $w_k^{b,1} = 0.005$ for $k > 1$. We consider $N_s = 81$ time steps in the simulation and the trajectories shown in Figure 2.

The field of view covers the range interval $[r_{min}, r_{max}] = [10, 300]$ and all possible direction of arrivals. Clutter intensity $\lambda^C(\cdot)$ is uniform such that

$$\lambda^C\left(\left[z_1^T, z_2\right]^T\right) = \overline{\lambda}^C \mathcal{V}\left(z_1; [1, 0]^T, 0\right) u_{[r_{min},, r_{max}]}(z_2) \tag{46}$$

where $\overline{\lambda}^C = 10$ is the mean number of clutter measurements per scan, $u_{[r_{min}, r_{max}]}(\cdot)$ is a uniform density in the interval $[r_{min}, r_{max}]$. If a measurement z belongs to the field of view, we have $\lambda^C(z) = \overline{\lambda}^C (r_{max} - r_{min})^{-1}$.

The probability of detection is

$$p_D(x) = \exp\left(-\frac{r(x)}{3 r_{max}}\right). \tag{47}$$

C. Results

We evaluate the error of estimating the set of targets at each time step by computing the root mean square generalised optimal subpattern assignment (RMS-GOSPA) metric [44], and its decomposition into localisation errors for properly

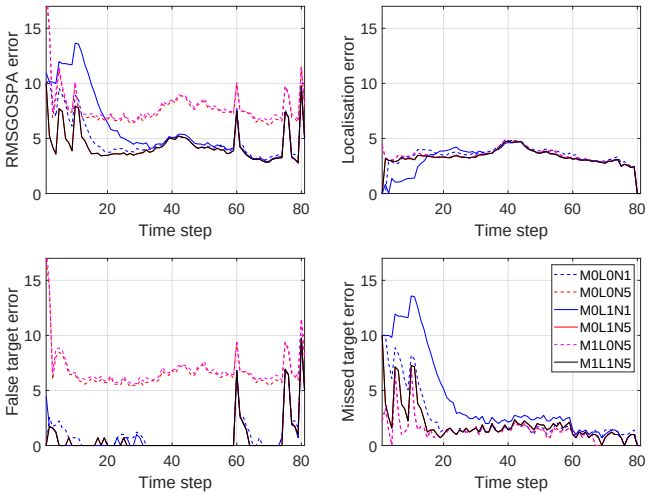

Figure 3: RMS-GOSPA error against time and its decomposition for the different PMBM filter variants: measurement driven linearisation initialisation (M1), standard intialisation (M0), normalising constant improvement (L1), standard normalising constant estimation (L0), number N_{iplf} of IPLF iterations (NN_{iplf}). The variants with 5 iterations and likelihood improvement perform best. The plots for M1L1N5 and M0L1N5 overlap. The variant with M1L1N1, not shown in the figure, behaves similarly to M1L1N5 and M0L1N5.

detected targets, costs for false targets and costs for missed targets considering 200 Monte Carlo runs. The GOSPA metric has been used with parameters $\alpha = 2$, $p = 2$ and $c = 10$. The RMS-GOSPA metric errors against time and their decomposition are shown in Figure 3 for Gaussian range and several variants of the approaches to approximate the single-target posteriors and normalising constants.

The best performing approximations are M1L1N1, M1L1N5 and M0L1N5. This indicates that the improvement of the normalising constant approximation and IPLF iterations, or measurement driven initial linearisation, are important factors to improve performance. The measurement-driven initial linearisation for new Bernoulli components has the effect of speeding up convergence time of the IPLF. Otherwise, we require several iterations of the IPLF to attain the same performance. The method conventionally used in the literature, M0L0N1, shows worse performance than the previous approximation schemes, especially in terms of missed targets. Using IPLF iterations without using the marginal likelihood improvement is detrimental due to an increase in false targets.

We proceed to provide a more thorough analysis, including results for Student's t range and the (track-oriented) Poisson multi-Bernoulli (PMB) filter [9]. For both types of range measurements, simulations are obtained by drawing samples from the corresponding distribution. The PMB filter is implemented with the same parameters as the PMBM filter, with a projection of the PMBM posterior to a PMB density with Gaussian single-target densities after each update step.

We show the resulting RMS-GOSPA errors across all time steps and their decompositions in Table I. As before, this table shows that the best performing approximations correspond to M1L1N1, M1L1N5 and M0L1N5, in combination with the PMBM filter for both Gaussian and Student's t range. The previous approach in the literature M0L0N1 shows higher errors, mainly attributed to an increase in false and missed targets for both types of range distributions. We can also see that the errors of the filters tend to be lower with the Gaussian range than with the Student's t. This is to be expected as the Student's t has longer tails which make tracking more complicated.

VI. Conclusions

In this paper, we have presented a Gaussian filtering method for multi-target tracking to deal with a state-dependent probability of detection and non-linear, non-Gaussian measurement models, described by their conditional moments. Measurement modelling via conditional moments allows us to develop Gaussian multiple target tracking algorithms for a broad class of measurement models, including von Mises-Fisher and Student's t-distribution. To deal with strong nonlinearities, we use the iterated posterior linearisation filter for the single-target updates and we approximate the normalising constant via sigma-point integration w.r.t. the posterior.

For updating the information on targets that have never been detected (PPP part in the PMBM filter) with large spatial uncertainty, we have introduced the use of a measurement-driven initial linearisation to speed-up the convergence of the iterated posterior linearisation filter. The proposed methods can be directly extended for multi-target tracking algorithms based on sets of trajectories [45].

A possible line of future work is to develop methods to take into account a state-dependent probability of detection to compute the Gaussian posteriors. This can be useful in situations where the probability of detection varies significantly in the area where the posterior has non-negligible mass.

References

[1] J. Choi, S. Ulbrich, B. Lichte, and M. Maurer, "Multi-target tracking using a 3D-lidar sensor for autonomous vehicles," in *16th International IEEE Conference on Intelligent Transportation Systems*, 2013, pp. 881–886.

[2] E. F. Brekke *et al.*, "The Autosea project: Developing closed-loop target tracking and collision avoidance systems," *Journal of Physics: Conference Series*, vol. 1357, pp. 1–12, Oct. 2019.

[3] E. Delande, J. Houssineau, J. Franco, C. Frueh, D. Clark, and M. Jah, "A new multi-target tracking algorithm for a large number of orbiting objects," *Advances in Space Research*, vol. 64, pp. 645–667, 2019.

[4] P. Braca, P. Willett, K. LePage, S. Marano, and V. Matta, "Bayesian tracking in underwater wireless sensor networks with port-starboard ambiguity," *IEEE Transactions on Signal Processing*, vol. 62, no. 7, pp. 1864–1878, Apr. 2014.

[5] D. Reid, "An algorithm for tracking multiple targets," *IEEE Transactions on Automatic Control*, vol. 24, no. 6, pp. 843–854, Dec. 1979.

[6] C.-Y. Chong, S. Mori, and S. Coraluppi, "Forty years of multiple hypothesis tracking," *Journal of Advances in Information Fusion. Special Issue on Multiple Hypothesis Tracking.*, vol. 14, no. 2, pp. 131–151, Dec. 2019.

[7] T. Fortmann, Y. Bar-Shalom, and M. Scheffe, "Sonar tracking of multiple targets using joint probabilistic data association," *IEEE Journal of Oceanic Engineering*, vol. 8, no. 3, pp. 173 –184, Jul. 1983.

[8] R. P. S. Mahler, *Advances in Statistical Multisource-Multitarget Information Fusion*. Artech House, 2014.

[9] J. L. Williams, "Marginal multi-Bernoulli filters: RFS derivation of MHT, JIPDA and association-based MeMBer," *IEEE Transactions on Aerospace and Electronic Systems*, vol. 51, no. 3, pp. 1664–1687, July 2015.

Table I: RMS-GOSPA errors and their decompositions

Range			Gaussian								Student's t							
Filter			PMBM				PMB				PMBM				PMB			
M	L	N_{iplf}	Tot.	Loc.	Fal.	Mis.	Tot.	Loc.	Fal.	Mis.	Tot.	Loc.	Fal.	Mis.	Tot.	Loc.	Fal.	Mis.
1	1	1	4.62	3.37	1.88	2.53	4.70	3.54	2.11	2.26	4.99	3.71	1.92	2.73	5.07	3.88	2.31	2.29
1	1	5	4.62	3.37	1.88	2.53	4.72	3.55	2.13	2.26	4.99	3.70	1.91	2.74	5.06	3.89	2.30	2.29
1	0	1	7.28	3.57	6.08	1.81	7.23	3.60	6.07	1.58	7.71	3.90	6.39	1.84	7.62	3.92	6.36	1.53
1	0	5	8.17	3.48	7.18	1.74	8.08	3.63	7.07	1.48	8.67	3.83	7.58	1.77	8.52	4.00	7.38	1.44
0	1	1	6.71	3.30	1.94	5.51	6.74	3.90	2.31	4.98	6.54	3.68	1.91	5.06	6.24	4.07	2.35	4.11
0	1	5	4.62	3.37	1.88	2.53	4.72	3.55	2.13	2.26	4.99	3.70	1.91	2.74	5.06	3.89	2.30	2.29
0	0	1	5.27	3.56	1.98	3.34	5.33	3.63	2.41	3.07	5.56	3.84	2.00	3.49	5.49	3.88	2.43	3.02
0	0	5	7.94	3.49	6.91	1.74	7.84	3.63	6.79	1.48	8.39	3.83	7.25	1.76	8.26	4.00	7.09	1.44

[10] E. Brekke and M. Chitre, "Relationship between finite set statistics and the multiple hypothesis tracker," *IEEE Transactions on Aerospace and Electronic Systems*, vol. 54, no. 4, pp. 1902–1917, Aug. 2018.

[11] M. Arulampalam, S. Maskell, N. Gordon, and T. Clapp, "A tutorial on particle filters for online nonlinear/non-Gaussian Bayesian tracking," *IEEE Transactions on Signal Processing*, vol. 50, no. 2, pp. 174–188, Feb. 2002.

[12] A. Gning *et al.*, "The effect of state dependent probability of detection in multitarget tracking applications," in *Proc. SPIE 9089*, 2014, pp. 1–12.

[13] N. Whiteley, S. Singh, and S. Godsill, "Auxiliary particle implementation of probability hypothesis density filter," *IEEE Transactions on Aerospace and Electronic Systems*, vol. 46, no. 3, pp. 1437–1454, July 2010.

[14] Y. Bar-Shalom, T. Kirubarajan, and X. R. Li, *Estimation with Applications to Tracking and Navigation*. John Wiley & Sons, Inc., 2001.

[15] S. J. Julier and J. K. Uhlmann, "Unscented filtering and nonlinear estimation," *Proceedings of the IEEE*, vol. 92, no. 3, pp. 401–422, Mar. 2004.

[16] I. Arasaratnam and S. Haykin, "Cubature Kalman filters," *IEEE Transactions on Automatic Control*, vol. 54, no. 6, pp. 1254–1269, June 2009.

[17] I. Arasaratnam, S. Haykin, and R. Elliott, "Discrete-time nonlinear filtering algorithms using Gauss-Hermite quadrature," *Proceedings of the IEEE*, vol. 95, no. 5, pp. 953–977, May 2007.

[18] S. Särkkä, *Bayesian Filtering and Smoothing*. Cambridge University Press, 2013.

[19] T. Lefebvre, H. Bruyninckx, and J. De Schuller, "Comment on "a new method for the nonlinear transformation of means and covariances in filters and estimators" [and authors' reply]," *IEEE Transactions on Automatic Control*, vol. 47, no. 8, pp. 1406–1409, Aug. 2002.

[20] T. Lefebvre, H. Bruyninckx, and J. D. Schutter, "Kalman filters for nonlinear systems: a comparison of performance," *International Journal of Control*, vol. 77, no. 7, pp. 639–653, May 2004.

[21] M. R. Morelande and A. F. García-Fernández, "Analysis of Kalman filter approximations for nonlinear measurements," *IEEE Transactions on Signal Processing*, vol. 61, no. 22, pp. 5477–5484, Nov. 2013.

[22] B. Bell and F. Cathey, "The iterated Kalman filter update as a Gauss-Newton method," *IEEE Transactions on Automatic Control*, vol. 38, no. 2, pp. 294–297, Feb. 1993.

[23] A. F. García-Fernández, L. Svensson, M. R. Morelande, and S. Särkkä, "Posterior linearization filter: principles and implementation using sigma points," *IEEE Transactions on Signal Processing*, vol. 63, no. 20, pp. 5561–5573, Oct. 2015.

[24] F. Tronarp, A. F. García-Fernández, and S. Särkkä, "Iterative filtering and smoothing in non-linear and non-Gaussian systems using conditional moments," *IEEE Signal Processing Letters*, vol. 25, no. 3, pp. 408–412, March 2018.

[25] D. Alspach and H. Sorenson, "Nonlinear Bayesian estimation using Gaussian sum approximations," *IEEE Transactions on Automatic Control*, vol. 17, no. 4, pp. 439–448, Aug. 1972.

[26] K. Ito and K. Xiong, "Gaussian filters for nonlinear filtering problems," *IEEE Transactions on Automatic Control*, vol. 45, no. 5, pp. 910–927, May 2000.

[27] Y. Bar-Shalom, F. Daum, and J. Huang, "The probabilistic data association filter," *IEEE Control Systems Magazine*, vol. 29, no. 6, pp. 82–100, Dec. 2009.

[28] S. Maresca, P. Braca, J. Horstmann, and R. Grasso, "Maritime surveillance using multiple high-frequency surface-wave radars," *IEEE Transactions on Geoscience and Remote Sensing*, vol. 52, no. 8, pp. 5056–5071, Aug. 2014.

[29] B.-N. Vo and W.-K. Ma, "The Gaussian mixture probability hypothesis density filter," *IEEE Transactions on Signal Processing*, vol. 54, no. 11, pp. 4091–4104, Nov. 2006.

[30] D. Macagnano and G. T. Freitas de Abreu, "Adaptive gating for multitarget tracking with Gaussian mixture filters," *IEEE Transactions on Signal Processing*, vol. 60, no. 3, pp. 1533–1538, 2012.

[31] M. Ulmke, O. Erdinc, and P. Willett, "GMTI tracking via the Gaussian mixture cardinalized probability hypothesis density filter," *IEEE Transactions on Aerospace and Electronic Systems*, vol. 46, no. 4, pp. 1821–1833, Oct. 2010.

[32] A. F. García-Fernández, F. Tronarp, and S. Särkkä, "Gaussian process classification using posterior linearization," *IEEE Signal Processing Letters*, vol. 26, no. 5, pp. 735–739, May 2019.

[33] V. Elvira, L. Martino, and P. Closas, "Importance Gaussian quadrature," *IEEE Transactions on Signal Processing*, vol. 69, pp. 474–488, 2021.

[34] A. F. García-Fernández, J. L. Williams, K. Granström, and L. Svensson, "Poisson multi-Bernoulli mixture filter: direct derivation and implementation," *IEEE Transactions on Aerospace and Electronic Systems*, vol. 54, no. 4, pp. 1883–1901, Aug. 2018.

[35] K. V. Mardia and P. E. Jupp, *Directional Statistics*. John Wiley & Sons, 2000.

[36] A. F. García-Fernández, F. Tronarp, and S. Särkkä, "Gaussian target tracking with direction-of-arrival von Mises-Fisher measurements," *IEEE Transactions on Signal Processing*, vol. 67, pp. 2960–2972, June 2019.

[37] B. O. Anderson and J. B. Moore, *Optimal Filtering*. Prentice-Hall, 1979.

[38] B. Ristic, D. Clark, B.-N. Vo, and B.-T. Vo, "Adaptive target birth intensity for PHD and CPHD filters," *IEEE Transactions on Aerospace and Electronic Systems*, vol. 48, no. 2, pp. 1656–1668, April 2012.

[39] A. F. García-Fernández, M. R. Morelande, J. Grajal, and L. Svensson, "Adaptive unscented Gaussian likelihood approximation filter," *Automatica*, vol. 54, pp. 166–175, April 2015.

[40] C. P. Robert and G. Casella, *Monte Carlo Statistical Methods*. Springer Science + Business Media, 2004.

[41] M. R. Morelande, "Tracking multiple targets with a sensor network," in *9th International Conference on Information Fusion*, July 2006, pp. 1–7.

[42] K. G. Murty, "An algorithm for ranking all the assignments in order of increasing cost." *Operations Research*, vol. 16, no. 3, pp. 682–687, 1968.

[43] S. Kotz and S. Nadarajah, *Multivariate t Distributions and Their Applications*. Cambridge University Press, 2004.

[44] A. S. Rahmathullah, A. F. García-Fernández, and L. Svensson, "Generalized optimal sub-pattern assignment metric," in *20th International Conference on Information Fusion*, 2017, pp. 1–8.

[45] A. F. García-Fernández, L. Svensson, and M. R. Morelande, "Multiple target tracking based on sets of trajectories," *IEEE Transactions on Aerospace and Electronic Systems*, vol. 56, no. 3, pp. 1685–1707, Jun. 2020.

Supplementary material "A Gaussian filtering method for multi-target tracking with nonlinear/non-Gaussian measurements"

APPENDIX A

For completeness, this appendix reviews how to select the sigma-points using the unscented transform [15], which is the method of choice in our simulations. Given (1), we choose $m = 2n_x + 1$ sigma-points $\mathcal{X}_0, ..., \mathcal{X}_{2n_x}$ with weights $\omega_0, ..., \omega_{2n_x}$ such that

$$\mathcal{X}_0 = \overline{x} \tag{48}$$

$$\mathcal{X}_i = \overline{x} + \left(\sqrt{\frac{n_x}{1-\omega_0}P}\right)_i \tag{49}$$

$$\omega_i = \frac{1-\omega_0}{2n_x} \tag{50}$$

$$\mathcal{X}_{i+n_x} = \overline{x} - \left(\sqrt{\frac{n_x}{1-\omega_0}P}\right)_i \tag{51}$$

$$\omega_{i+n_x} = \frac{1-\omega_0}{2n_x} \tag{52}$$

where $i = 1, ..., n_x$, ω_0 is a parameter that corresponds to the weight of the sigma point located at $\overline{x}$, and $\left(\sqrt{P}\right)_i$ is the ith column of the Cholesky decomposition of P, where $P = \sqrt{P}\left(\sqrt{P}\right)^T$.

APPENDIX B

In this appendix, we provide the required moments of $g(\cdot)$ and $R(\cdot)$, see (8), to perform SLR, see (15)-(18), for the range-bearings measurements in Section V-A. The expressions for Gaussian range and Student's t range are given in Section B-A and Section B-B, respectively.

A. Gaussian range

If the range has Gaussian density (40), and the direction-of-arrival measurement has VMF density (36), the moments of $g(\cdot)$ and $R(\cdot)$ can be obtained as [36]

$$\mathrm{E}\left[g\left(x\right)\right] = \left[A_2\left(\kappa\right)\mathrm{E}\left[h(x)\right]^T, \mathrm{E}\left[r(x)\right]\right]^T \tag{53}$$

$$\mathrm{C}\left[x, g\left(x\right)\right] = \left[A_2\left(\kappa\right)\mathrm{C}\left[x, h(x)\right], \mathrm{C}\left[x, r(x)\right]\right] \tag{54}$$

$$\mathrm{C}\left[g\left(x\right)\right] = \begin{bmatrix} \left(A_2\left(\kappa\right)\right)^2 \mathrm{C}\left[h(x)\right] & A_2\left(\kappa\right)B \\ A_2\left(\kappa\right)B^T & \mathrm{C}\left[r(x)\right] \end{bmatrix} \tag{55}$$

$$\mathrm{E}\left[R\left(x\right)\right] = \mathrm{diag}\left(\frac{A_2\left(\kappa\right)}{\kappa}I_2 + \left[1 - A_2^2\left(\kappa\right) - 2\frac{A_2\left(\kappa\right)}{\kappa}\right] \times \mathrm{E}\left[h\left(x\right)h^T\left(x\right)\right], R\right) \tag{56}$$

where

$$A_n\left(\kappa\right) = \frac{\mathrm{I}_{n/2}\left(\kappa\right)}{\mathrm{I}_{n/2-1}\left(\kappa\right)} \tag{57}$$

$$B = \mathrm{C}\left[h(x), r\left(x\right)\right]. \tag{58}$$

It is also possible to select the enabling approximation (10) independently for each sensor [32], [36], which is more suitable for a large number of sensors. For large κ, there can be numerical inaccuracies to calculate $A_n\left(\kappa\right)$ and $\mathrm{I}_{n/2-1}\left(\kappa\right)$, which can be avoided by using their asymptotic approximations [35, Eq. (10.3.5)-(10.3.6)]. The moments of $h\left(x\right)$ and $r\left(x\right)$ in (53)-(56) can be approximated using sigma-points.

B. Student's t range

The conditional moments of the Student's t range measurement z_2 given the state, see (41), are

$$\mathrm{E}\left[z_2|x\right] = r\left(x\right), \quad \nu > 1 \tag{59}$$

$$\mathrm{C}\left[z_2|x\right] = \frac{\nu}{\nu-2}R, \quad \nu > 2. \tag{60}$$

We therefore require $\nu > 2$ such that both conditional moments are defined and we can apply the filters based on conditional moments.

Equations (59) and (60) imply that the cross-moments (53)-(55) remain unchanged for Student's t range, and (56) becomes

$$\mathrm{E}\left[R\left(x\right)\right] = \mathrm{diag}\left(\frac{A_2\left(\kappa\right)}{\kappa}I_2 + \left[1 - A_2^2\left(\kappa\right) - 2\frac{A_2\left(\kappa\right)}{\kappa}\right] \times \mathrm{E}\left[h\left(x\right)h^T\left(x\right)\right], \frac{\nu}{\nu-2}R\right). \tag{61}$$